

Evaluation of Neutron and Proton Nuclear Data of ^{28}Si for Energies up to 200 MeV

Sun Weili¹, Y. Watanabe², E. Sh. Sukhovitskiĭ³, O. Iwamoto⁴, and S. Chiba⁴

¹*Department of Applied Quantum Physics and Nuclear Engineering, Kyushu University, Fukuoka 812-8581, Japan*

²*Department of Advanced Energy Engineering Science, Kyushu University, Kasuga, Fukuoka 816-8580, Japan*

³*Radiation Physics and Chemistry Problems Institute, 220109, Minsk-Sosny, Belarus*

⁴*Japan Atomic Energy Research Institute, Tokai-mura, Naka-gun, Ibaraki-ken, 319-1195, Japan*
e-mail: sun@aes.kyushu-u.ac.jp

The neutron and proton nuclear data of ^{28}Si up to 200 MeV are evaluated for various nuclear engineering applications. The soft rotator model and the coupled-channel method are used to perform a consistent analysis of the collective band structure of ^{28}Si and nucleon scattering from ^{28}Si . The GNASH nuclear model code is used for compound and preequilibrium particle emission calculations, where the emission of ^3He is also included. Comparisons show overall good agreement with various experimental data.

1. Introduction

Recently, neutron and proton nuclear data in the intermediate energy range are required in various fields related to advanced sciences and technologies, such as accelerator-driven transmutation of nuclear waste, cancer therapy and soft-error evaluation in computer memories. From the viewpoint of applications, nucleon-induced nuclear data of silicon are of importance since silicon is a major component of shielding materials and memory chips in computers. To meet these needs, the neutron and proton nuclear data of ^{28}Si are evaluated up to 200 MeV, based on the measured data as well as nuclear model predictions.

Since ^{28}Si is considered to be as a deformed nucleus with a rotational structure, the coupled-channel (CC) method with a coupling based on the wave functions of soft rotator model, developed by Minsk group[1], is used to perform a consistent analysis of the collective band structure and nucleon scattering. A very interesting characteristic of this model is that the nuclear Hamiltonian parameters for nuclear wave functions are adjusted first to reproduce the experimentally observed low-lying collective structure, and then these functions will be used to construct the coupling scheme for CC calculations. With the applications to a light nucleus, ^{12}C [2], an intermediate heavy nucleus ^{58}Ni [3], and heavy (actinide) nuclei[4], this model shows its success and high accuracy in describing nuclear structure, nucleon scattering and spectroscopic data in a uniform approach. It is, therefore, expected that such a consistent analysis will create a reliable and high accurate evaluation for ^{28}Si .

2. Coupled-Channel Calculations

This work has used the soft rotator model including nonaxial quadrupole, octupole, and hexadecapole deformation, and the β_2 , β_3 , and γ vibration, where the symbols and definitions are same as those in Refs. [2, 3].

By giving suitably an initial assignment of quantum numbers to low-lying levels, the SHEM-MAN code[5] is used to adjust the nuclear Hamiltonian parameters to describe ten experimental

levels. The final parameters and the predicted level scheme are given in Table 1 and Fig. 1, respectively. Note that only six predicted levels with spins and parities as 0_1^+ , 2_1^+ , 4_1^+ , 0_2^+ , 2_2^+ , and 3_1^- are plotted. These levels are coupled most strongly, and are used in CC calculations as described below. It is seen that these levels are predicted well within 10-15 % accuracy.

The wave functions with those adjusted Hamiltonian parameters are used to construct the coupling scheme among the six levels, as shown in Fig. 2, in the CC calculations using OPTMAN code[5]. The present calculation, as did in the previous works [2, 3], has considered that the each level is coupled not only with all other levels, but also with itself. The Coulomb interaction enhances the coupling in all the pairs of the levels except between 0^+ (g.s) and 0_2^+ (4.9798 MeV). These two levels are coupled only by nuclear potential, due to the account of nuclear charge conservation which leads to the truncation of Coulomb potential zero multipoles.

The optical model parameters are searched by minimizing the quantity χ^2 to fit best to the experimental data. To describe the scattering data at higher energies, the simple exponential energy dependence of spin-orbit potential suggested by dispersion relationship is taken into account. The best fitted parameters are given in Table 2. Fig.3-6 show that the total and proton reaction cross sections as well as nucleon scattering data are predicted well by the present model parameters in a consistent way. One can see that the predictions for the proton elastic scattering data over 100 MeV, as shown in right panel of Fig. 5, show some oscillating patterns at backward angles. The reason might be due to the use of simple energy dependence of potential, which make the adjustment of parameters over a wide range of incident energies very difficult. On the the hand, the calculation underestimates the neutron inelastic scattering on 2^+ at 14.2 MeV. This may be because the compound inelastic scattering processes are not included in the calculations.

3. Particle Emission Calculations

The GNASH[6] nuclear reaction model code is used for calculations of compound and preequilibrium particle and γ -ray emissions. Six light particles, n , p , d , t , ^3He and α , are taken into account. The transmission coefficients are required in these calculations. A method of connecting the CC method and Hauser Feshbach theory in terms of generalized transmission coefficients was proposed by Ohsawa[7]. In the present work, $T_\ell^{(cc)}(\varepsilon)$ obtained from the above-mentioned CC calculations are used for the entrance channel. Note that this results in use of a compound formation cross section without the contributions from direct inelastic cross sections. For the exit channels of neutron and proton, renormalized transmission coefficients, $T_\ell(\varepsilon) \approx \sigma_r(\varepsilon)/[\sigma_r(\varepsilon) - \sigma_{dir}(\varepsilon)]T_\ell^{(cc)}(\varepsilon)$, are used, where $\sigma_r(\varepsilon)$ is the total reaction cross section, and $\sigma_{dir}(\varepsilon)$ the sum of all direct inelastic cross sections. This renormalization leads to approximate use of spherical optical model transmission coefficients.

The Wilmore-Hodgson [8] and Becchetti-Greenlees [9] potentials are used for lower neutron and proton energies (<20 MeV), respectively. They give an approximate continuity in reaction cross sections to those by the potentials in Table.2. The Daehnick potential [10] is used for deuteron, Becchetti-Greenlees potential for triton and ^3He , and Avrigeanu potential[11] for alpha particle. The level densities of Ignatyuke et al.[12] are used for all residual nuclei, except the level density parameters of ^{28}Si ($a=3.35 \text{ MeV}^{-1}$, $\Delta=3.89 \text{ MeV}$), ^{28}Al ($a=3.55$, $\Delta=0$), and ^{25}Mg ($a=4.325$, $\Delta=1.75$), which are taken as those of Bateman [13].

Figures 7-9 show comparisons of energy spectra, double differential cross sections (DDXs), and isotope production cross sections with experimental data and those from the evaluated data library ‘‘LA150’’[14]. It is obvious that all spectra and DDXs have an evaporation peak from compound processes at lower emission energy, and a smooth high energy tail from preequilibrium processes. The present results describe overall good agreement with the experimental data.

Figure 9 shows such an example where the QMD calculations at higher energies (200 MeV-

Table 1: The Hamiltonian parameters used to reproduce the experimental level scheme.

$\hbar\omega_0 = 4.218$	$\mu_{\beta_{20}} = 0.6299$	$\mu_{\gamma_0} = 0.727$	$\gamma_0 = 0.3706$	$a_{32} = 0.0$	$a_{42} = 0.01997$
$\delta_4 = 0.6858$	$\gamma_4 = 0.03269$	$\mu_\epsilon = 0.1274$	$\eta = 0.1346$	$\delta_n = 4.092$	

Table 2: The optical potential parameters allowing the best fit of the experimental data. Strength and incident energy E in MeV; radii and diffusenesses in fm.

$V_R=54.21-0.288E+0.0004E^2$			
$W_D = 0.46+0.225E$	$E \leq 19.85$ MeV		
$=4.926-0.0507(E-19.85)$	$E > 19.85$ MeV		
$W_V = 0.1046+0.152E$	$E \leq 19.85$ MeV		
$=3.122+0.0954(E-19.85)$	$E > 19.85$ MeV		
$V_{SO}=4.43e^{0.005E}$	$W_{SO}^0=0.69$	$W_{SO}^1=-0.00211$	
$r_R=1.1207$	$a_R=0.644+0.00003E$		
$r_D=1.2897$	$a_D=0.37+0.0052E$	$E \leq 19.85$ MeV	
	$=0.4732$	$E > 19.85$ MeV	$C_{Coul}=0.662$
$r_V=1.0719$	$a_V=0.49+0.0018E$		$\beta_{20}=0.414$
$r_{SO}=1.0987$	$a_{SO}=0.618$		$\beta_{30} = \beta_{20}\epsilon_0=0.215$
$r_C=1.1298$	$a_C=0.872$		$\beta_4=0.0622$

3 GeV) are given and has a good continuity at 200 MeV to those results by the GNASH code. Note that the experimental data are those for natural silicon. The present results include only the data for ^{28}Si , while those of LA150 and QMD include both data for ^{28}Si and natural silicon.

In conclusions, the present consistent analysis of collective structure and nucleon scattering data, based on the soft rotator model, describe the experimental levels and nucleon scattering data well. The present evaluations show the overall agreement with experimental energy spectra, DDX and production cross sections, and as well as LA150.

Our next step is planned to include the calculations of double differential recoil spectra of heavy reaction products.

References

- [1] Y. V. Porodzinski \tilde{i} and E. Sh. Sukhovitski \tilde{i} , Sov. J. Nucl. Phys. **53**, 41 (1991); Sov. J. Nucl. Phys. **54**, 941 (1991).
- [2] S. Chiba et al., Nucl. Phys. **A624**, 305 (1997).
- [3] E. Sh. Sukhovitski \tilde{i} et al., Phys. Rev. **C62**, 044605 (2000).
- [4] Y. V. Porodzinski \tilde{i} and E. Sh. Sukhovitski \tilde{i} , Phys. At. Nucl. **59**, 244 (1996).
- [5] E. Sh. Sukhovitski \tilde{i} et al., Report No. JAERI-Data/Code 98-019, JAERI, 1998.
- [6] P. G. Young et al., Proc. IAEA Workshop Nucl. Reaction Data and Nucl. reactor -Physics, Design, and Safety, Triest, Italy, April 15- May 17, 1996, p.227
- [7] T. Ohsawa et al., Proc. Int. Conf. Nucl. Data for Basic and Appl. Sci., Santa Fe, May 1985, p. 1193.
- [8] D. Wilmore and P. E. Hodgson, Nucl. Phys. **55**, 673 (1964).
- [9] F. D. Becchetti and G. W. Greenlees, Proc. Conf. Polarization Phenomena in Nuclear Reactions, p. 682 (1971).

- [10] B. Daehnick et al., Phys. Rev. **C21**, 2253 (1980).
- [11] V. Avrigeanu et al., Phys. Rev. **C49**, 2136 (1994).
- [12] A. V. Ignatyuke et al., Sov. J. Nucl. Phys. **21**, 255 (1975).
- [13] F. B. Bateman et al., Phys. Rev. **C60**, 064609 (1999).
- [14] M. B. Chadwick et al., Nucl. Sci. Eng. **131**, 293 (1999).

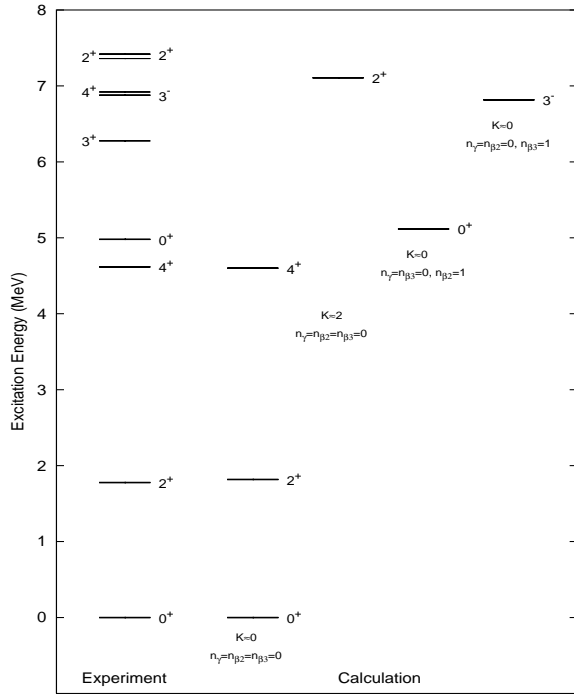


Figure 1. Comparison of the experimental and calculated level schemes. Thick lines show experimental levels described by the soft rotator model.

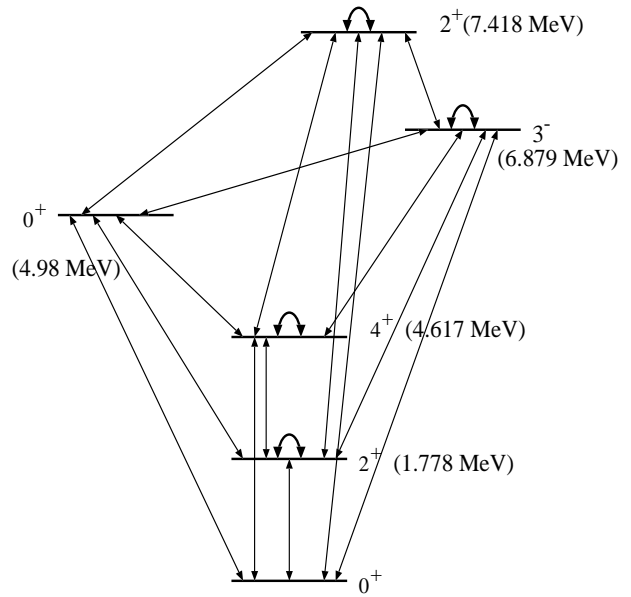


Figure 2. Coupled scheme employed in the present calculations. Arrows show the coupling used in the parameter search procedure.

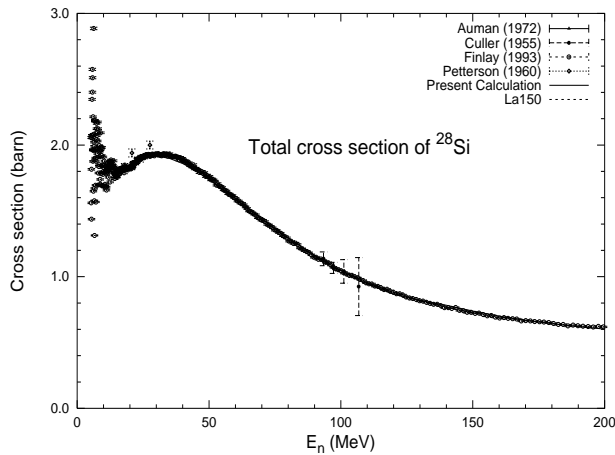


Figure 3. Comparison of the calculated total cross sections with experimental data and evaluated data from LA150.

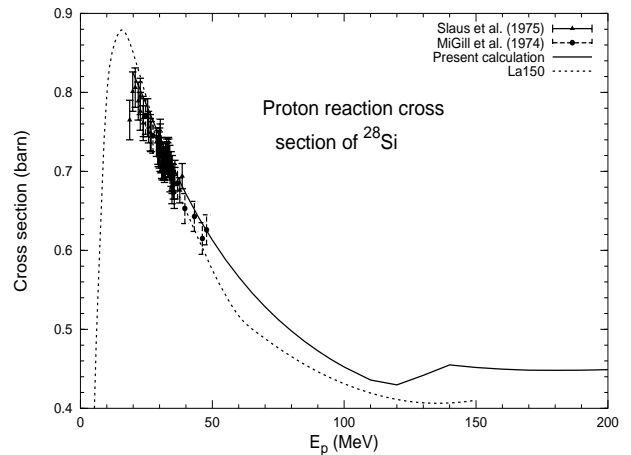


Figure 4. Comparison of the calculated proton reaction cross sections with experimental data and LA150. The present calculations do not give the cross sections for lower energies (< 20 MeV).

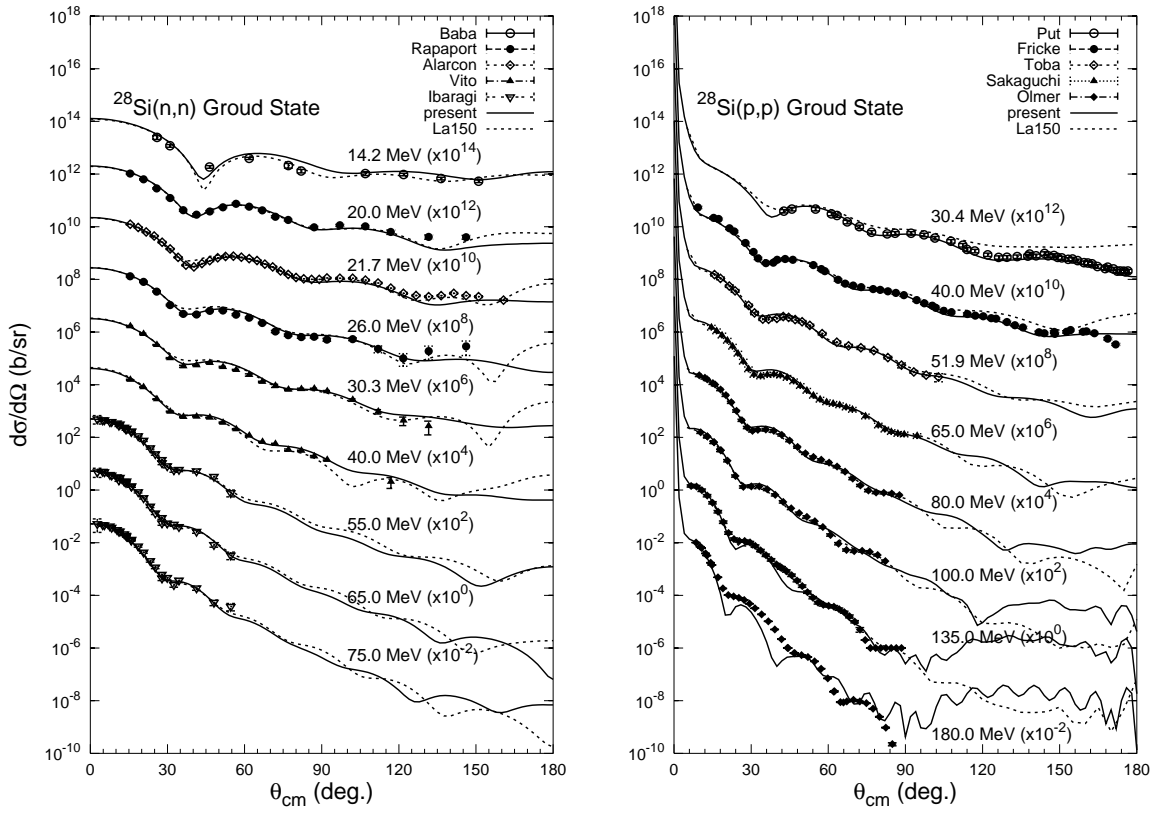


Figure 5. Comparison of the elastic scattering angular distribution with experimental data and LA150.

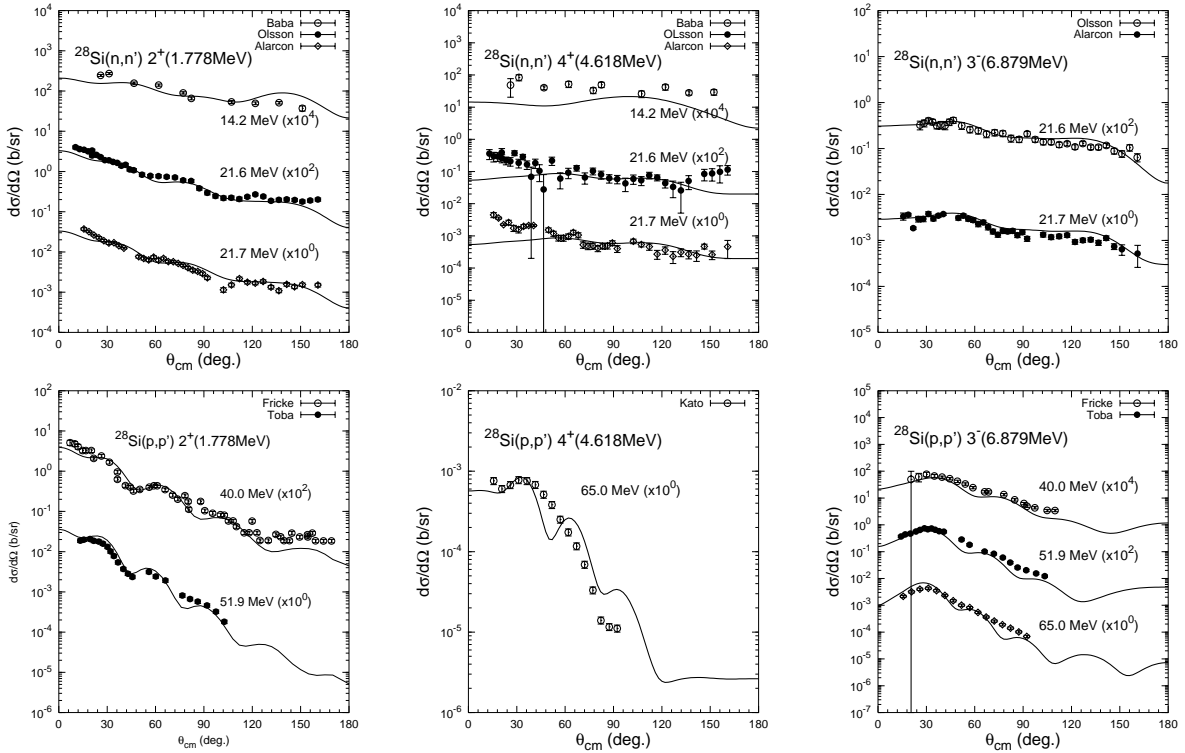


Figure 6. Comparison of the inelastic scattering angular distributions with experimental data.

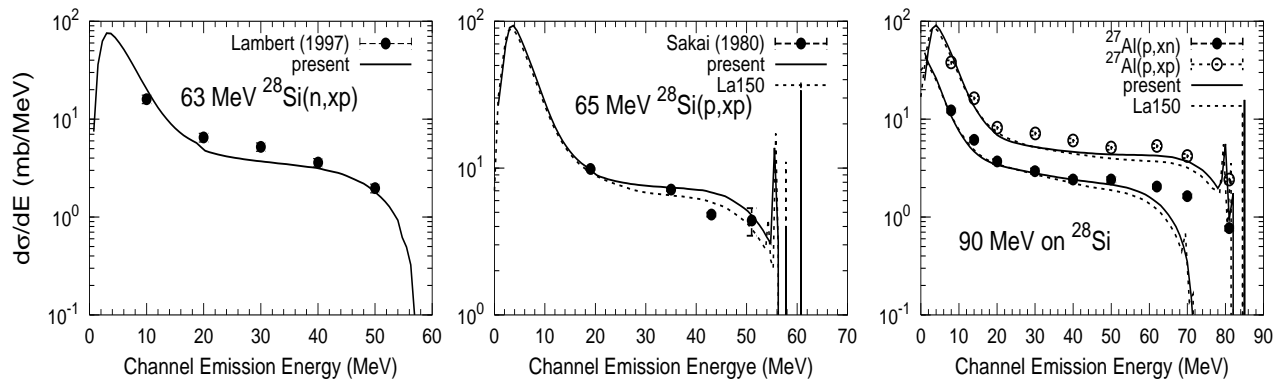


Figure 7. The emitted particle energy spectra of (n, xp) , (p, xn) and (p, xp) reactions, compared with experimental data and LA150. The (p, xn) and (p, xp) data at 90 MeV are taken from $p+^{27}\text{Al}$ reaction scaled by $A^{2/3}$.

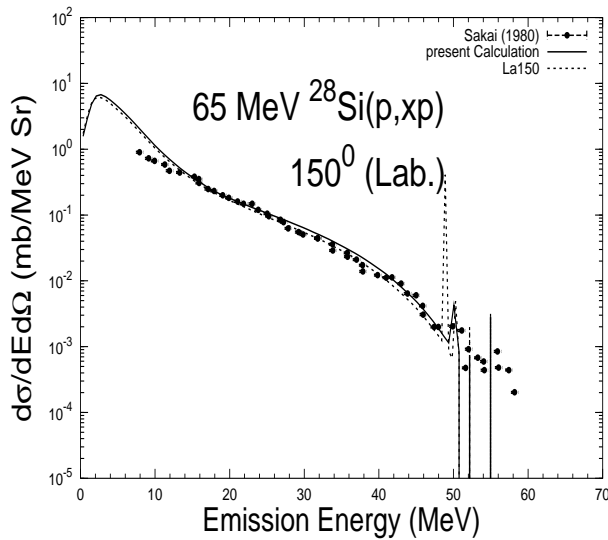


Figure 8. The double differential cross sections at 150° for $^{28}\text{Si}(p, xp)$ reaction, compared with experimental data and LA150.

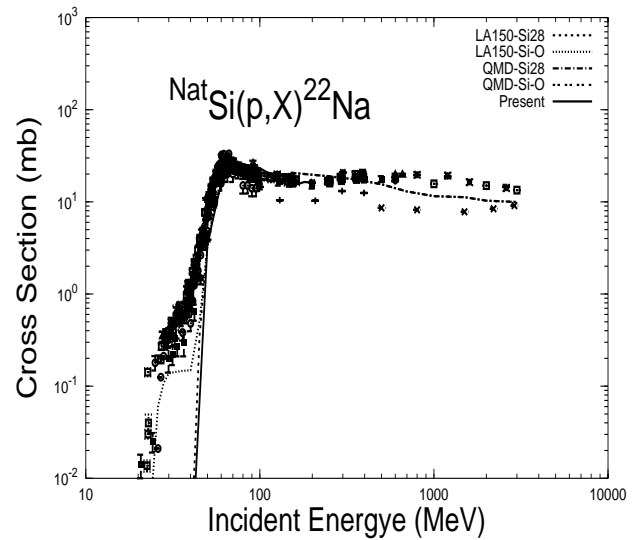


Figure 9. The production cross sections for ^{22}Na , compared with experimental and LA150. The experimental data are those for natural silicon. The present calculations give only the results for ^{28}Si , while the LA150 gives the results for ^{28}Si and natural silicon. The QMD calculations are also presented to show the continuity at 200 MeV to the results of GNASH calculations. All symbols are experimental data taken from EXFOR.